

## Article

# Geological and Geomorphological Context and Characterization of Constructive Materials from the Iberian–Roman Archaeological Site at La Vispesa (NE Spain)

José Luis Peña-Monné <sup>1,\*</sup>, María Marta Sampietro-Vattuone <sup>2</sup>, Elena Maestro-Zaldívar <sup>3</sup> and Almudena Domínguez-Arranz <sup>3</sup>

<sup>1</sup> Departamento de Geografía y Ordenación del Territorio, Universidad de Zaragoza y Real Academia de Ciencias Exactas, Físicas Químicas y Naturales de Zaragoza, 50009 Zaragoza, Spain

<sup>2</sup> Laboratorio de Geoarqueología, Universidad Nacional de Tucumán y CONICET, San Miguel de Tucumán 4000, Argentina; sampietro@tucbbs.com.ar

<sup>3</sup> Departamento de Ciencias de la Antigüedad, Universidad de Zaragoza, 50009 Zaragoza, Spain; emastro@unizar.es (E.M.-Z.); almodin@unizar.es (A.D.-A.)

\* Correspondence: jlpena@unizar.es

## Abstract

La Vispesa is an archaeological settlement occupied from the First Iron Age to the Imperial Roman Period. The objectives of this study were to (i) perform a geomorphological characterization of the site; (ii) place it in its regional context; (iii) obtain values of uniaxial compressive strength (UCS) to characterize the construction materials; (iv) assess the chronological data obtained; (v) establish the origin of the sandstones used; and (vi) assess the application of these techniques at archaeological sites. UCS estimations were produced for the preserved walls using a Schmidt hammer, and two groups of samples were identified. In these samples, stones from the Iberian Epoch walls were considerably weathered, while the Roman ashlar were well preserved as they were built from better-quality material that produced high UCS values. In addition, measurements of various sandstone outcrops probably used as quarries were made to compare values. Only one sandstone outcrop had estimations that could relate to the provision of raw material for the Roman period, while other estimations are compatible with Iberian walls. The application of this methodology proves to be highly beneficial for the analysis and comprehension of ancient constructions.

**Keywords:** geomorphology; geoarchaeology; Schmidt hammer; weathering; archaeology



Received: 3 June 2025  
Revised: 19 June 2025  
Accepted: 23 June 2025  
Published: 25 June 2025

**Citation:** Peña-Monné, J.L.; Sampietro-Vattuone, M.M.; Maestro-Zaldívar, E.; Domínguez-Arranz, A. Geological and Geomorphological Context and Characterization of Constructive Materials from the Iberian–Roman Archaeological Site at La Vispesa (NE Spain). *Heritage* **2025**, *8*, 248. <https://doi.org/10.3390/heritage8070248>

**Copyright:** © 2025 by the authors. Licensee MDPI, Basel, Switzerland. This article is an open access article distributed under the terms and conditions of the Creative Commons Attribution (CC BY) license (<https://creativecommons.org/licenses/by/4.0/>).

## 1. Introduction

The La Vispesa archaeological site is located near Binéfar in the province of Huesca in the northeast of the Iberian Peninsula (Figure 1a). It is situated on an isolated hill at an elevation of 292.6 m a.s.l. with wide views over the surrounding plains (Figure 1b). The region was part of the of the Ilergetan territory between ca. 500 and 200 BC, reaching its greatest development during the third century BC. From the second century BC, it became part of the Tarraconensis Province. Several archaeological excavations carried out between 1984 and 2005 led to the discovery of a *castellum* from the Late Republican Roman Period, overlapping an earlier *oppidum* from the Iberian (Ilergetan) Period [1–5]. The two construction stages are well-defined from both stratigraphic and archaeological perspectives. Even at the first glance, the construction phases can be identified, as the structural elements exhibit varying degrees of conservation. This difference cannot be

attributed solely to chronological factors, given the minimal temporal separation between the two stages. Additionally, petrographic and mineralogical data indicate a high degree of homogeneity in the composition of these walls and the rocky outcrops of the surroundings [6,7]. Thus, a Schmidt hammer (SH) was used to test the ashlars and stones of the walls to determine the characteristics of the sandstone used in both periods, as well as to study nearby outcrops of the same lithology. This method does not damage the archaeological remains and provides data on the degree of rock weathering based on the resistance to uniaxial compression (UCS).

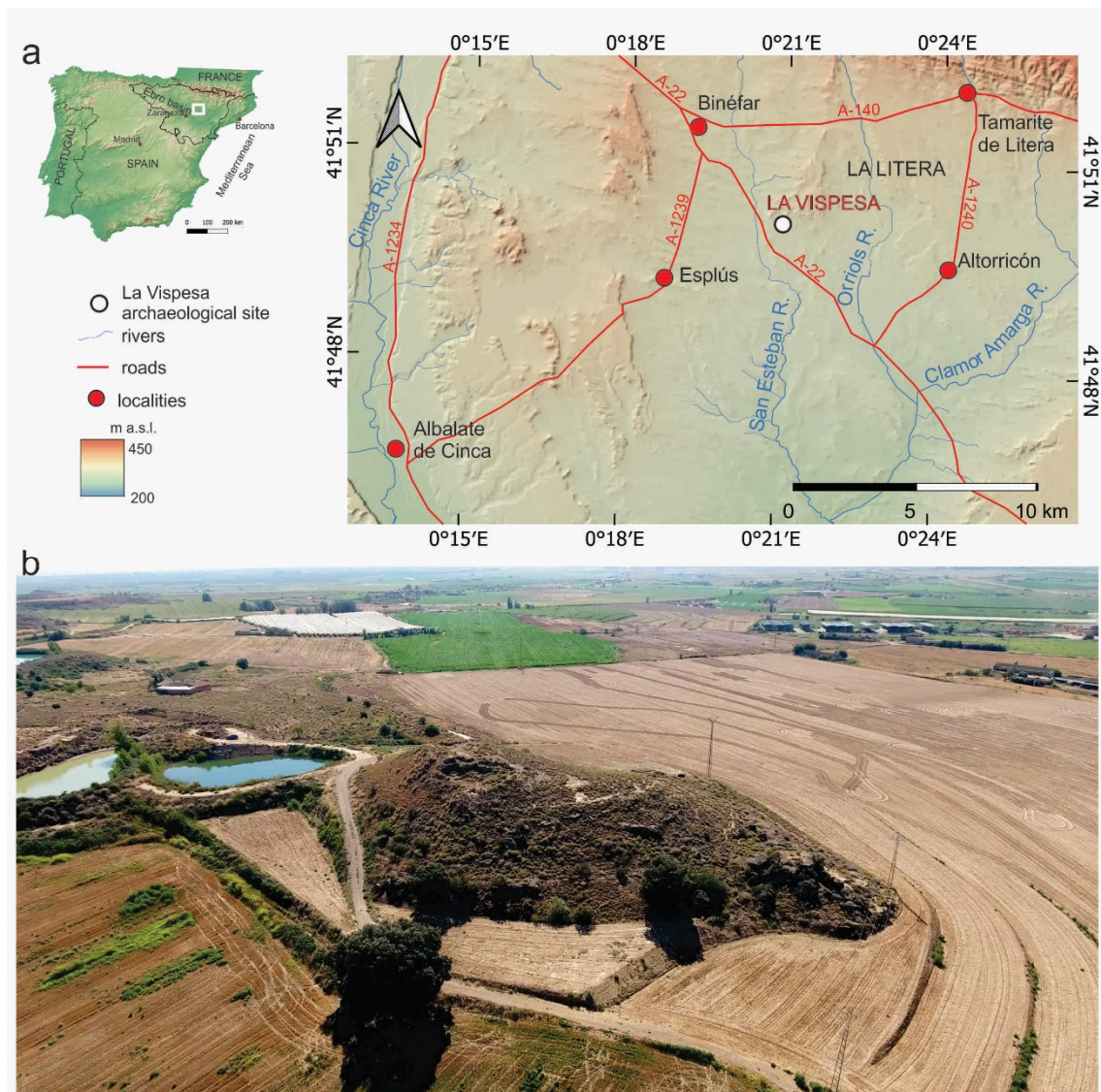


**Figure 1.** (a) Location map of La Vispesa; (b) oblique aerial photograph of La Vispesa Hill and the plain of La Litera from the northwest.

The SH is primarily used to assess the strength of concrete walls, but it is also applied in geotechnical studies, following specific standards [8–11]. Furthermore, it has been employed in geomorphological research to estimate the relative ages of large blocks in accumulations, such as glacier moraines, by evaluating degrees of weathering ([12] in Scandinavia, [13] in the Pyrenean Range). Recently, it was applied to study the evolution of sandstone escarpments in Los Monegros (central sector of the Ebro Depression) using measurements from detached blocks to estimate relative chronologies [14]. However, no comparable studies were identified in archaeological contexts that analyze the origin of

ashlar and stone raw materials and the timing of their use in construction among rocks with similar lithologies.

The objectives of this paper are (a) to place the archaeological site within its geological and geomorphological contexts; (b) to create a detailed geomorphological map to highlight the main characteristics of the site and locate potential raw material sources; (c) to determine the UCS of the sandstone ashlar and stones used in the walls of La Vispesa for each occupational period; (d) to identify differences in the properties and weathering of the sandstone to verify the established chronologies; (e) to compare these findings with nearby sandstone outcrops to locate potential quarries; and (f) to assess the usefulness of this method for identifying preferences for various raw materials used in constructions across cultural groups or periods.

### 1.1. Geographical and Geological Settings

The La Vispesa archaeological site is located in the Aragonese region of La Litera (*La Llitera*) within the municipality of Tamarite de Litera, near the border with Catalonia. Geologically, it is part of the eastern–central sector of the Ebro Depression (Figure 1a). This tectonic trench formed as a foreland basin during the Alpine orogenic phases, coinciding with the rise of the Pyrenean Mountain Range. Throughout the Cenozoic, it was filled as an endorheic basin with detrital and evaporite deposits forming the so-called “Huesca fans” [15,16]. The sedimentary materials of the La Litera region belong to the Sariñena Fm [17,18] and are dated to the Chattian–Aquitainian ages [19]. These deposits consist of marls and clays with interbedded sandstones and microconglomerates.

The sandstone composition of the Sariñena Fm was defined by [15] and in detail by [20,21]. According to the classification of [20], it is a lithic arenite or litharenite. It exhibits a heterometric framework composed of calcite grains (50–52%), dolomite (34–36%), and, to a lesser extent, quartz (12–13%) and phyllosilicates (3–4%), cemented by calcite. The open porosity ranges between 4.9% and 6.1%, facilitating water infiltration and subsequent physico-chemical weathering. The compositional homogeneity is consistent throughout the middle/distal zone of the Sariñena Formation, complicating the mineralogical and petrographic differentiation of both outcrops and construction materials derived from this lithology.

During the Quaternary, the area located between the Noguera Ribagorzana, Segre, and Cinca rivers experienced extensive erosion, resulting in a topographic depression amidst older and higher Quaternary river terraces. The fluvial network primarily drained through the Clamor Amarga and Sosa rivers (tributaries of the Cinca River). Part of the older Quaternary deposits in the La Litera region originated from the Sosa River, which was later captured by the middle section of the Cinca River in the Monzón area, along with other fluvial courses like Orriols and San Esteban. These rivers created pediments and alluvial fans with gentle gradients extending towards the S and SE, which formed a stepped pattern at different accumulation levels. During the Upper Pleistocene, as the channels of the Cinca and Segre rivers became entrenched, secondary watercourses caused intense erosion, reducing early accumulations to isolate *mesas* and form residual hills. The La Vispesa archaeological site is located on one of these hills (Figure 1b).

The climate is continental Mediterranean with semi-arid characteristics. The average annual temperature and rainfall are 14.4 °C and 383 mm, respectively (data from Binéfar station). The region experiences a significant annual water deficit. These semi-arid conditions leave the area prone to high rates of erosion. Additionally, centuries of overgrazing and agriculture have affected the surroundings of La Vispesa, leading to the development of steppe vegetation. This vegetation, except on shaded slopes, offers little protection against soil erosion.

### 1.2. La Vispesa Archaeological Site

La Vispesa is one of the locations that has provided extensive information about the processes of Iberization and Romanization in the region, along with significant movable and immovable remains [1,2,21]. The archaeological findings belong to an Ibero-Roman settlement located on the hill's summit and its surrounding plain, dating from the First Iron Age (Ilergetan Period) to the Roman Imperial Period.

Two primary and stratigraphically overlapping periods of occupation have been identified: a large Iberian *oppidum* and a Roman *mansio* associated with the road connecting Ilerda and Osca. These settlement phases reached their peak during the third and second centuries BC for the former and the second and first centuries BC for the latter (Figure 2).

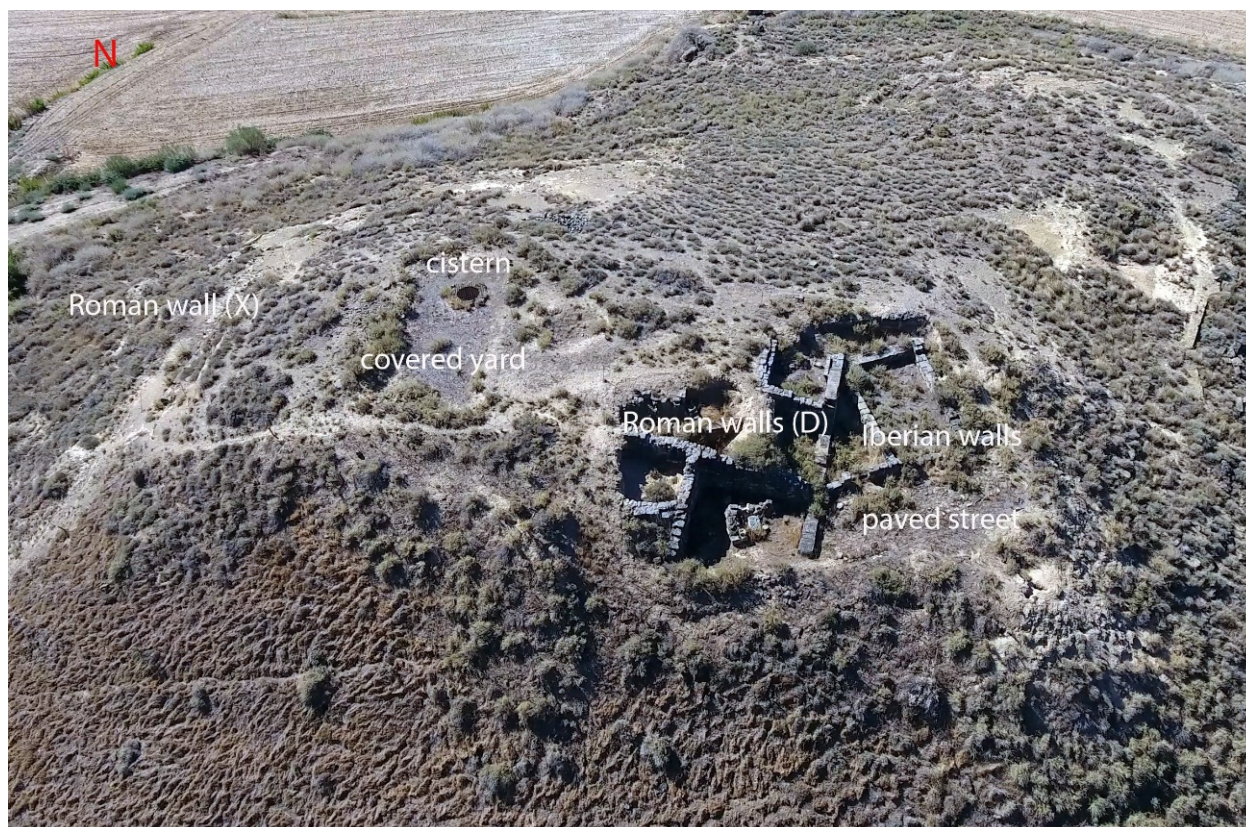


**Figure 2.** Main archaeological areas of the La Vispesa site.

The site was abandoned after Romanization and not reoccupied. Recently, the remains of the Ilergetan settlement and parts of a unique Republican building have been consolidated to prevent deterioration [4]. These remains are located at the top of the hill and on its slopes, although the Iberian settlement extended to the plain.

The Iberian residences follow a quadrangular layout, with sandstone stone foundations joined with clay and mud. Above these foundations, walls were built using adobe and rammed earth. Floors were made of compacted earth and lime. Streets were adapted to the terrain's contours, and only one street preserved its original stone slab paving. This first settlement is dated to the third century BC, during the Full Iberian period. Between 100 and 75 BC, some of the Iberian residences on the slopes were used as quarries to construct Roman buildings at the hilltop. The land was leveled, and a robust structure was erected, including a cistern (or well) to collect rainwater in one of its rooms.

Additionally, the site has yielded epigraphic and archaeological remains related to Iberian religious beliefs, as well as numerous ceramic fragments and coins. These finds hold significant archaeological value, enhancing our understanding of Ibero-Roman culture and its connections with contemporary Mediterranean societies [5,21]. One of the most notable discoveries is the Binéfar Stele [22], renowned for its exceptional iconographic and artistic richness and now housed in the Huesca Museum. The stele may have belonged to a building or temple dedicated to the indigenous deity Neitin.

## 2. Methodology

A geomorphological map, scale 1:1000, was drawn to show the most characteristic geological and geomorphological features of the site and its surroundings. The graphical representation was made following the proposal of [23] for detailed geomorphological maps. As base documents, an orthoimage and DEM calculated from SfM photogrammetry were used. Vertical images were taken at 100 m height with an FC220 camera (12.4 Mpx) on a UAV DJI Phantom 4. The remote control was programmed in Android using Pix4DCapture, and 134 photographs that overlapped 80% were obtained. Images were processed with Agisoft Metashape Professional v.1.5.1. Oblique photographs and videos were taken.

Petrographic, geochemical, and isotopic analyses are commonly carried out to determine the provenance of building materials at archaeological sites (see, for example, [24–26]). However, given the difficulty in compositional differentiation of the sandstones that make up the walls of La Vispesa, we tested the use of a non-invasive method based on the comparison of estimated uniaxial compressive strength (UCS) values. The hardness or resistance measurements of the sandstone blocks, ashlars, and paleochannels were made using a sclerometer (Ectha 1000 Schmidt hammer (SH) Diagnostic Research Company, Los Angeles, CA, USA). Rebound values were obtained following [8,10] from the International Society for Rock Mechanics (ISRM), as well as [27,28] for geomorphological applications. Twelve sampling points were established with 20 rebound (R) measurements taken at each point. Large blocks were selected (more than 30 cm along the A axis) with smooth uncracked surfaces at least 50 cm above the soil surface to avoid weathering bias caused by capillarity. In one case, measurements were made for different orientations to determine the relevance of this factor. Another six sampling points were established on different paleochannels of the same hill. The estimations of UCS were assessed using the Miller index [29] to estimate how much the rocks had weathered. Data were analyzed by calculating the descriptive statistical parameters to establish the range, mean, and medium—and represented in a box and whisker chart, following the proposal of [14]. Rock densities were determined by weighing the samples, and their volumes were estimated using water displacement with the results expressed in  $\text{kg}/\text{m}^3$ .

## 3. Results

The hill over which La Vispesa is settled has an N-S elongated shape (Figures 1b and 3). It is one of the several residual reliefs scattered in the La Litera plain. It is composed of gravels from various lithologies (Figure 4a) because part of the sediment originates from the erosion of the high terraces of the Cinca River and the conglomerates of the Pyrenean Marginal Ranges. At the top, the pediment displays a thick and hardened calcrete (Figure 4b), which is common in this type of accumulation, as well as in the old terraces of the main rivers [30,31]. Consequently, these carbonate hardenings generate reliefs that are highly resistant to erosion.

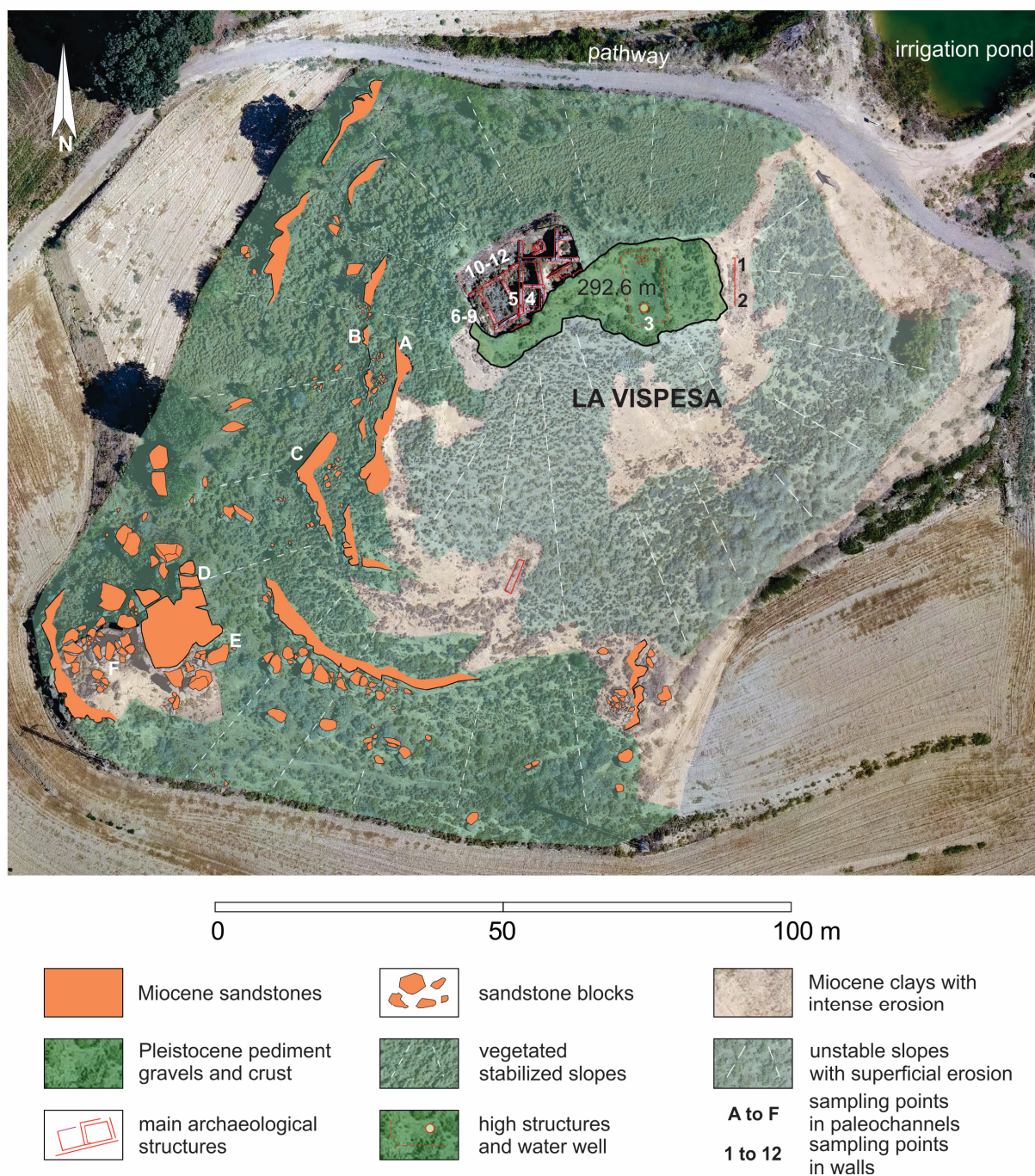


**Figure 3.** Geomorphological map of La Vispesa hill and Schmidt hammer sampling points' distribution.

At the foot of the pediments, gentle slopes are modeled in clays and marls of the Sariñena Fm, with small intermediate escarpments formed by outcrops of sandstones and microconglomerates (Figures 3 and 4c). A large escarpment on the S and SW faces of the hill stands out, with a thickness of over 3 m height (Figure 4d). In addition to these resistant levels, the slopes facing E and S exhibit intense erosion (Figure 3) caused by run-off due to sparse vegetation cover, which exposes the soft materials of Sariñena Fm. In contrast, the W-facing slope is more stable and the level of erosion has been diminished by vegetation (Figures 1b and 3). The arrangement displays a dissymmetrical morphology caused by the orientation of slopes. This setting corresponds to the context of the Ilergian and Roman occupations.

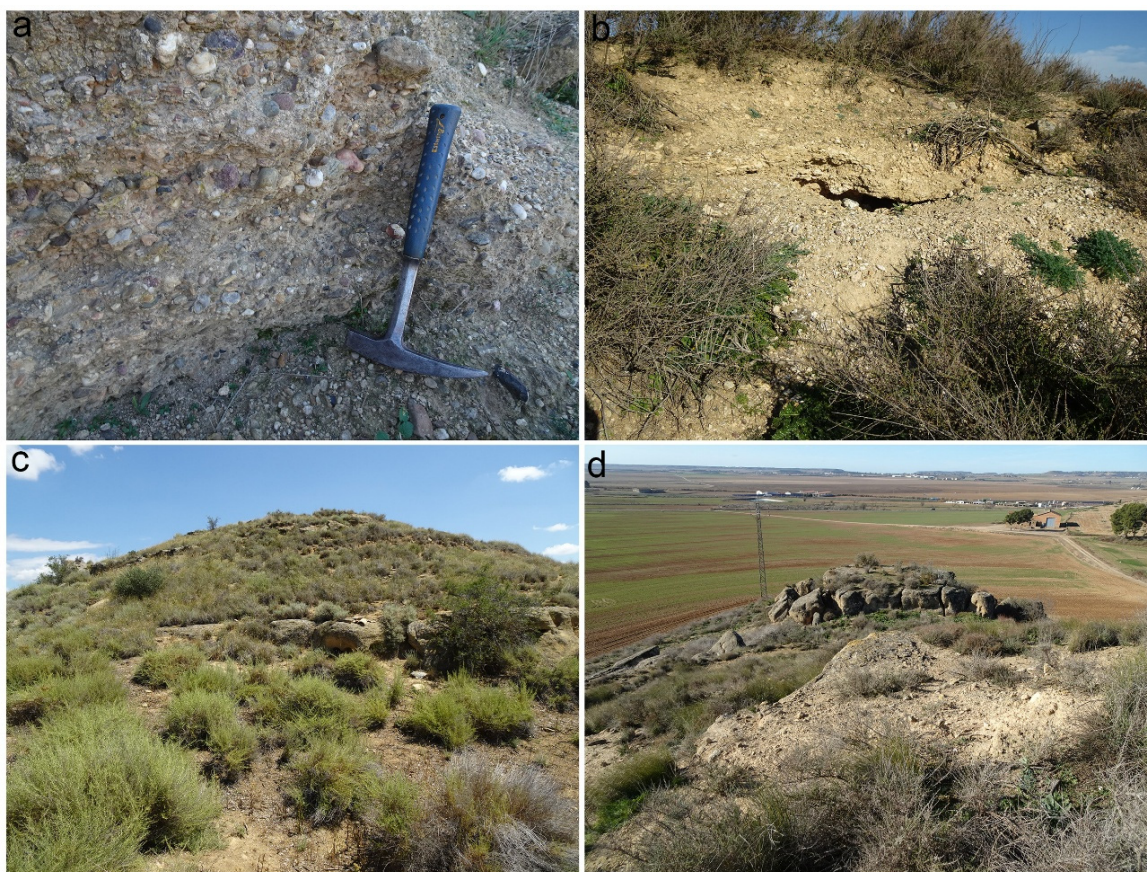


**Figure 4.** Lithological composition of La Vispesa hill; (a) polygenic gravels of the Pleistocene pediment that form the top escarpment in the area of the main excavation; (b) upper calcrete crust containing glacial gravels; (c) SW slope modeled over marls and clays with steps of sandstone paleochannels; (d) sandstone paleochannel relief from the SW face.

### 3.1. SH Rebound (R) Measurements and UCS Estimations of the Settlement Walls

Archaeological structures reveal two different types of constructive materials distinguishable by their morphologies. Roughly carved sandstone stones form part of the basement of the Iberian residences, while other stones and paving slabs are conserved in one of the streets. These constructions date to the Full Iberian Period, as noted by [2]. Many of these materials were later repurposed for the construction of the *opus vittatum* walls when consolidating and widening the upper platform during Roman Period [2,3]. Some of these walls also contain large, rounded gravels and blocks coming from the remains of the upper pediment.

In addition, there are large, well-squared quadrangular ashlar (*opus quadratum*), often featuring bossed surfaces, made of sandstones, measuring  $1 \times 0.5 \times 0.5$  m, which date back to the Roman Epoch (1st century BC). These ashlar are set transversely to the NE and W sides of the Iberian walls in a different direction to the pre-existing walls and probably marked the boundaries of the construction.

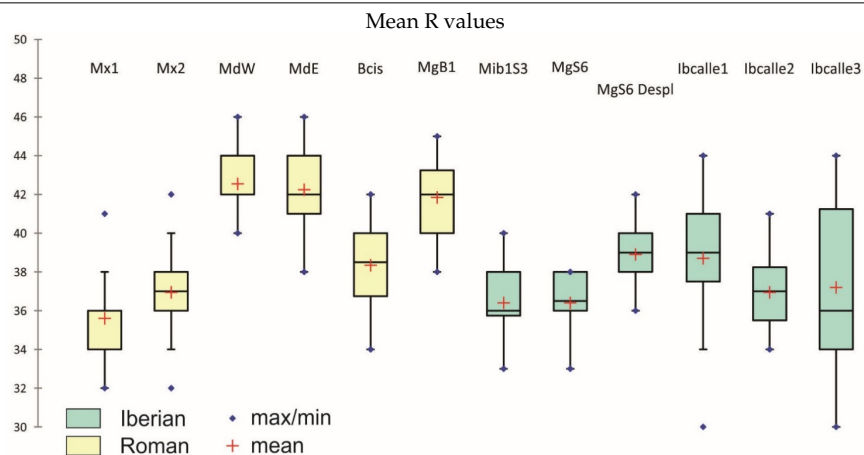
Twelve representative sample points from both buildings were selected to apply SH rebound (R) measurements (Figures 3 and 5). These include four sampling points on two Roman walls: two on wall X (Mx) of the eastern slope, and two on wall D (Md) within the main archaeological excavation on the western side. Additionally, sample were taken from an ashlar in the cistern area, as well as four stones from the Iberian walls, and three slabs from the Iberian street. The results are presented in Table 1, corresponding to the 12 sampled points in Figures 3 and 5.



Figure 5. Location of the SH sampling points at the archaeological site.

Table 1. Statistical data and graphical representation of the measurements obtained using a Schmidt hammer (SH) on walls from the Iberian and Roman periods.

| Statistics          | Mx1  | Mx2  | MdW   | MdE  | Bcis | MgB1 | Mib1S3 | MgS6 | MgS6 Despl | Ibcalle1 | Ibcalle2 | Ibcalle3 |
|---------------------|------|------|-------|------|------|------|--------|------|------------|----------|----------|----------|
| No. of observations | 20.0 | 20.0 | 20.0  | 20.0 | 20.0 | 20.0 | 20.0   | 20.0 | 20.0       | 20.0     | 20.0     | 20.0     |
| Minimum             | 32.0 | 32.0 | 40.0  | 38.0 | 34.0 | 38.0 | 33.0   | 33.0 | 36.0       | 30.0     | 34.0     | 30.0     |
| Maximum             | 41.0 | 42.0 | 46.0  | 46.0 | 42.0 | 45.0 | 40.0   | 38.0 | 42.0       | 44.0     | 41.0     | 44.0     |
| Range               | 9.0  | 10.0 | 6.0   | 8.0  | 8.0  | 7.0  | 7.0    | 5.0  | 6.0        | 14.0     | 7.0      | 14.0     |
| Median              | 36.0 | 37.0 | 42.0  | 42.0 | 38.5 | 42.0 | 36.0   | 36.5 | 39.0       | 39.0     | 37.0     | 36.0     |
| Mean                | 35.6 | 37.0 | 42.6  | 42.3 | 38.4 | 41.9 | 36.4   | 36.4 | 38.9       | 38.7     | 37.0     | 37.2     |
| Sd. deviat.         | 2.2  | 2.2  | 1.5   | 2.0  | 2.3  | 1.9  | 1.8    | 1.6  | 1.6        | 3.1      | 2.2      | 4.2      |
| UCS (MPa)           | 57.5 | 60.0 | 77.27 | 73.6 | 63.6 | 73.6 | 52.5   | 52.5 | 60.0       | 56.9     | 52.5     | 52.5     |



Two samples were taken from the large Roman ashlar of wall X (Mx1 and Mx2) on the south-facing side (Figure 6a) (the northern face is not exposed). The mean R values obtained were  $35.6 \pm 2.2$  and  $37 \pm 2.2$ , with ranges between 32 and 41–42 (Table 1). These ashlar show evident weathering traces, differentially affecting some inner layers with cross-bedding (Figure 6b), and joints among ashlar (Figure 6c). The density value was  $23.3 \text{ kg/m}^3$ . UCS estimations for the Mx set ranged from 57.5 to 60 MPa (Table 1). The

sample taken from the cistern ashlar (Bcis) (Figure 6d) gave an R value of  $38.34 \pm 2.3$  and UCS of 63.6 MPa, which are higher than those recorded for Mx (Table 1).



**Figure 6.** Different sampling points in the Roman walls: (a) wall X (Mx) with the sampled points; (b) selective weathering in the sandstone wall with cross-bedding (see the lower padded ashlars and chisel marks); (c) joints of the wall X showing weathering; (d) sampled ashlar of the cistern; (e) point MdW sampled in wall D of the primary excavation; (f) point MdE on the other side of the same ashlar.

In the main excavation, there is a sandstone wall (Md) that is similar to Mx. On one of the Md ashlars, rebound measurements (R) were taken with a Schmidt hammer on the western (MdW) (Figure 6e) and eastern faces (MdE) (Figure 6f). The mean R values obtained were  $42.6 \pm 1.5$  and  $42.3 \pm 2$ , showing consistent homogeneity in the maximum values (46/46) and minimum (40/38) values (Table 1). At first glance, both faces of these ashlars appear slightly weathered and chisel marks are clearly visible. These sandstone ashlars were previously buried beneath a sediment layer and were uncovered during the archaeological excavation. This condition may account for the differences when compared to the more weathered ashlars from wall X. The UCS values for wall D were 77.27 and 73.6 Mpa.

Three samples were taken from the stones of wall E, part of an Iberian residence (space E20) (Figure 7a). The first two samples (Mib1S3 and MgS6) (Figure 7b) show similar results, with R values of  $36.4 \pm 1.8$  and  $36.4 \pm 1.6$ , showing maximum values of 40/38 and a minimum of 33. The estimated density was  $22.3 \text{ kg/m}^3$  and the UCS value was 52.5 MPa. Another sample from the same wall (MgB1) was taken from a more finely carved block that was made of sandstone similar to the material used in Roman ashlars. This sample showed an R value of  $41.9 \pm 1.9$ , ranging between 45 and 38, with a UCS value of 73.6 MPa (Table 1). The sandstone type is consistent with that used during Roman times as the results are similar to wall D.



**Figure 7.** Sampling points in the Iberian walls: (a,b) western wall; (c,d) street slabs.

The surface weathering observed in the blocks of the mentioned Iberian residency (Figure 7a) can be estimated from the measurements of sample MgS6, which has a mean R value of  $36.4 \pm 1.6$  and a UCS of 52.5 MPa. Another sample (MgS6 Despl) was taken from the same stone in an area where spalling recently occurred. With the external layer removed, the rock is in a state closer to its original condition and yielded mean R values of  $38.9 \pm 1.6$  and a UCS of 60 MPa (Table 1). The difference between the values of the intact and spalled rock provides an estimate of the strength loss due to weathering since the Iberian period—calculated to be  $8 \text{ kg/m}^3$ .

Lastly, three measurements were also taken from the street pavement (Ibcalle1, Ibcalle2, Ibcalle3) (Figure 7c,d), and these yielded mean R values of  $38.7 \pm 3.1$ ,  $37 \pm 2.2$ , and  $37.2 \pm 4.2$ , respectively, with maximums ranging from 41 to 44 and minimums between 30 and 34. The UCS value obtained for the set was between 56.9 and 52.5 MPa.

### 3.2. Surrounding Sandstone Paleochannels: SH Rebound (R) Values and UCS

On the hill of La Vispesa, several sandstone and microconglomerate outcrops with paleochannel configurations can be found. The most continuous and thickest outcrops are located in the middle and lower sections of the southwestern (SW) and southeastern (SE) slopes of the hill (Figure 4c,d). Four paleochannels were selected to take rebound (R)

measurements. The aim is to compare these results with those obtained from the settlement walls to identify potential quarry sites for the two occupation phases.

The SH measurements (labeled A to F, Figure 3) were taken from the paleochannel closest to the hilltop down to the paleochannel adjacent to the cultivated area at the base (Figure 8a). Measurement A was taken from a 0.5 m thick sandstone layer with a very straight escarpment, as blocks were extracted from this paleochannel in 2000 to reinforce the archaeological structures. The mean R value recorded was  $36.1 \pm 1.7$ , with measurements ranging from 49 to 32, corresponding to a UCS of 54.4 MPa (Table 2). A few meters lower, another paleochannel (B) with a thickness of 0.75 m yielded a mean R value of  $35.9 \pm 1.7$  (with maximum and minimum values of 39 and 34, respectively). Based on the rock density, this measurement also corresponds to a UCS of 54.4 MPa—which is identical to previous results (Table 2).

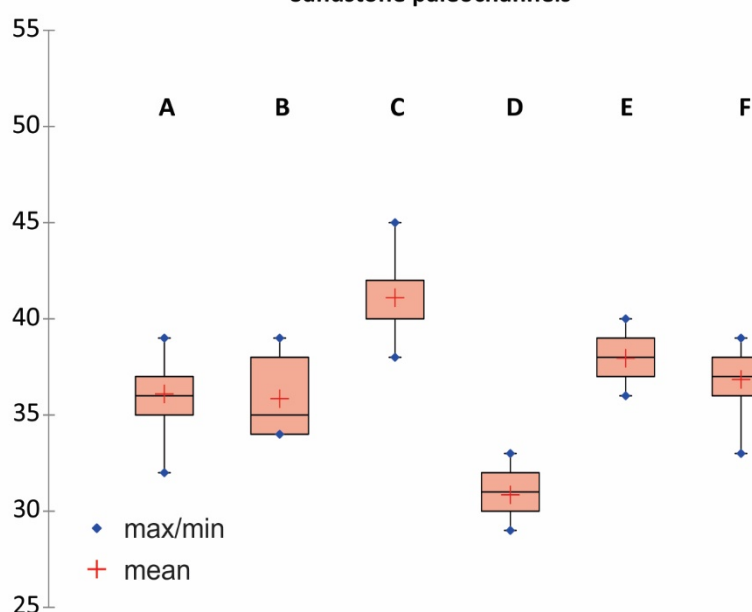


**Figure 8.** (a) SH measurements points on the sandstone paleochannels of La Vispesa; in yellow, location of images c, d, and e; (b) measurement of point C; (c) wedge marks in the vertical escarpment of paleochannel from point C; (d) extension of wedge marks on the surface of the same paleochannel; (e) possible ashlar extraction scarp; (f) paleochannel where samples D and E were taken.

**Table 2.** Statistical data and graphical representation of the measurements obtained using a Schmidt hammer (SH) on the sandstones in the La Vispesa area, and UCS estimates for potential quarry source for wall stones and ashlars.

| Statistics          | A    | B    | C    | D    | E    | F    |
|---------------------|------|------|------|------|------|------|
| No. of observations | 20.0 | 20.0 | 20.0 | 20.0 | 20.0 | 20.0 |
| Minimum             | 32.0 | 34.0 | 38.0 | 29.0 | 36.0 | 33.0 |
| Maximum             | 49.0 | 39.0 | 45.0 | 33.0 | 40.0 | 39.0 |
| Range               | 7.0  | 5.0  | 7.0  | 4.0  | 4.0  | 6.0  |
| Median              | 36.0 | 35.0 | 40.0 | 31.0 | 38.0 | 37.0 |
| Mean                | 36.1 | 35.9 | 41.1 | 30.8 | 37.9 | 36.8 |
| Sd. deviat.         | 1.7  | 1.7  | 2.0  | 1.0  | 1.0  | 1.5  |
| UCS (MPa)           | 54.4 | 54.4 | 75.5 | 44.0 | 52.8 | 53.8 |

Mean R values Sandstone paleochannels



Paleochannel C is thicker (1–2 m) than the previous two paleochannels and appears less weathered (Figure 8b), although some honeycombs (Figure 8c) and small alveoli are visible in certain parts of the escarpment. The mean R value was  $41.1 \pm 2$ , with measurements ranging between 45 and 38, and its UCS was estimated at 75.5 MPa (Table 2). Close to sampling point C (Figure 8a), wedge marks for block extraction were identified (Figure 8c), both on the vertical escarpment (seven marks approximately 20 cm long and 2–4 cm wide) and continuing on the paleochannel surface (with two marks of similar dimensions—Figure 8d). To the east, a section of sandstone with a very linear escarpment and a 90° notch (Figure 8e) can be observed that likely corresponds to another block extraction site. Other indications, such as stepped formations on the escarpment, can only be explained by the previous presence of a quarry. Both this escarpment and the identified marks show weathering processes indicative of ancient extractions.

The paleochannel where the remaining three SH measurements (D, E, F) were taken is the largest. It is a wide outcrop, measuring between 2.5 and 3 m, with a vertical escarpment and a flat surface. In some areas, conglomerates are exposed at its base, overlain by sandstones and microconglomerates that show fluvial structures and cross-bedding. A network of fractures facilitates the detachment of the paleochannel into numerous blocks, which are imbricated along the southwestern side. The northeastern escarpment has a

notably straight profile, which could be attributed to extraction activities. However, it also aligns with the trace of an orthogonal fracture that affects the rock. The presence of well-developed tafoni, with residual hardenings on the walls (Figure 8f), suggests that this linear feature is not the result of quarrying operations.

Measurements D and E yielded average R values of  $30.8 \pm 1$  and  $37.9 \pm 1$ , respectively, which differ significantly. Their corresponding UCS values are 44 MPa and 52.8 MPa. This difference may be attributed to their orientations: sample D is northeast-facing, while sample E faces southeast. Lastly, SH measurements were taken on the southwest-facing side of one of the blocks. The average R value was  $36.8 \pm 1.5$ , with a range between 39 and 33, corresponding to an estimated UCS of 53.8 MPa.

#### 4. Discussion

The geomorphological study of La Vispesa hill, particularly the detailed map, reveals a type of terrain that is typical in the central–eastern sector of the Ebro Depression. The asymmetry of the hill is also common in similar landforms (many of which are archaeological sites) such as the central hill within the archaeological complex of Moradilla (Lleida) [32], as well as other hills along the lower courses of the Cinca and Segre rivers [33]. Additional examples can also be found in the middle Ebro valley and in the Iberian Range [34].

Many of these residual and isolated landforms have served as the base for settlements in various periods due to their strategic importance. Their evolution begins with an initial mesa-like morphology, characterized by a summit and escarpment formed from remnants of Pleistocene glacial deposits composed of sub-rounded gravels cemented with a calcrete crust [14]. In some cases, fluvial terraces crown these landforms. The slopes of these summits have eroded over time, resulting in residual or witness hills. Ref. [35] classified the isolated hills in nearby areas, which are locally known as ‘tozales’ or ‘tossals’, depending on the region’s predominant language (Spanish or Catalan). La Vispesa corresponds to Type 2 in this evolutionary classification. Similar hills can be found in neighboring regions such as Los Monegros [14,35] and the surroundings of Lleida and Fraga [32]. These were primarily occupied during the Bronze Age and some were also used during the Medieval period.

According to ISRM standards, rocks are classified based on their UCS values, ranging from extremely hard (>250 MPa) to extremely soft (<1 MPa). The sandstones forming the construction structures of La Vispesa, based on HS measurements, belong to the hard rock category (50–100 MPa) (Table 1). Specifically, the sandstones from Roman wall D (MdW and MdE) and two Roman ashlar—one integrated into the Iberian wall (MgB1) and another near the cistern (Bcis)—exceed 60 MPa. In contrast, the stones from the Iberian residences and the Roman ashlar from wall X fall within the 50–60 MPa range.

The R results from the sandstone paleochannels resulted in four UCS values ranging between 50 and 60 MPa (samples A, B, E, F), with sample D slightly below this range. Only paleochannel C, which had a rebound value averaging 41.1, reached an estimated UCS of 75.5 MPa—remarkably high within the hard rock category. Additionally, this paleochannel features wedge marks for block extraction and straight walls with minimal signs of advanced weathering, and this suggests its use as a quarry.

By comparing the average R measurements with the estimated UCS values for La Vispesa in a single figure, it is possible to identify a relationship between the construction phases and the sandstone sources likely used for obtaining these materials (Figure 9). The four highest rebound and strength values clearly correspond to the Roman-crafted group, which aligns in UCS with the sandstone sample from paleochannel C. In contrast, Roman wall X and all the walls and pavements from the Iberian period show values that are more consistent with the remaining sandstone samples, which display lower rebound and UCS values.

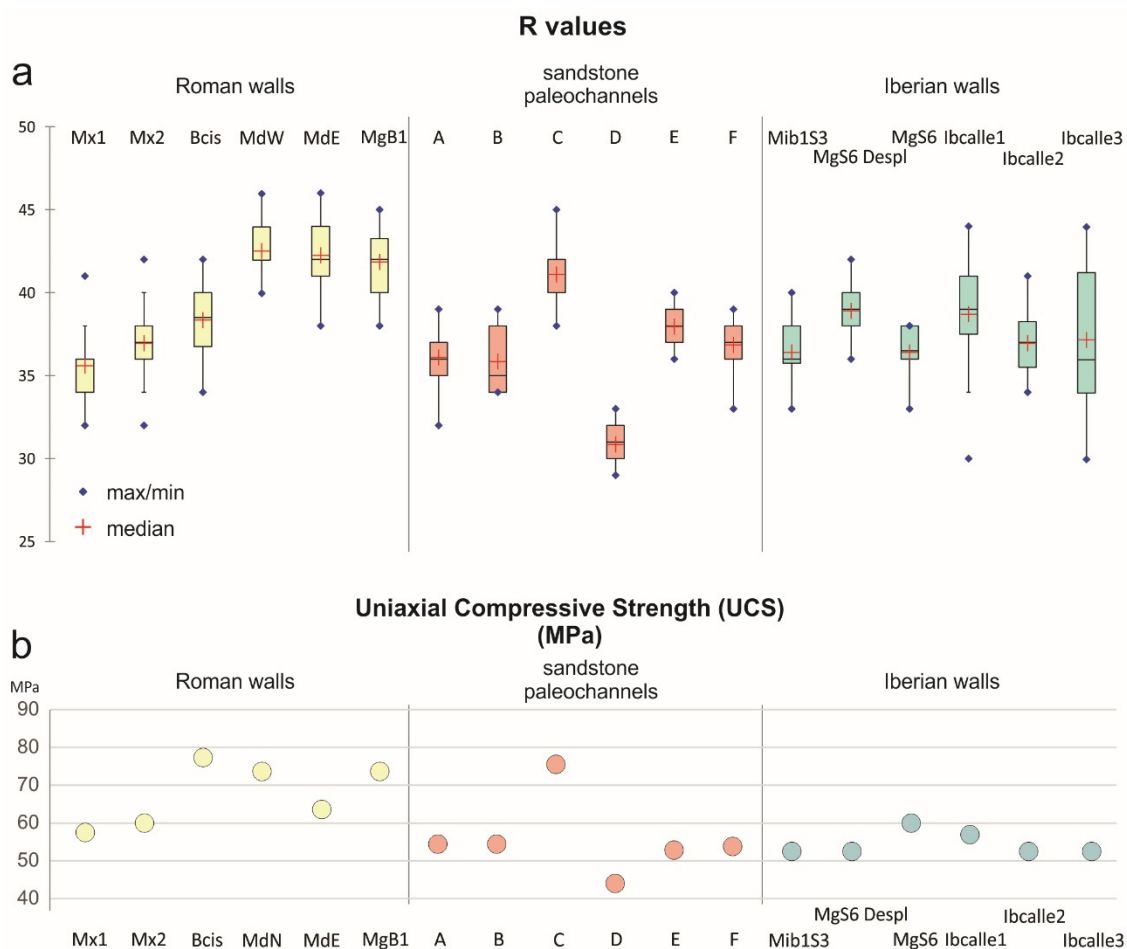


**Figure 9.** R values and UCS estimates from the Iberian and Roman walls and relation with sandstone paleochannels results in establishing potential quarries for the supply of blocks and ashlar. (a) box-and-whiskers plot; (b) uniaxial compressive strength results.

The large Roman ashlar, carved from fine-grained sandstone, demonstrate a much higher quality than the other construction materials. These blocks exhibit minimal or no internal fractures and few stratification lines, which would otherwise facilitate water infiltration and accelerate weathering. As can be seen in Figure 3, the distance between the paleochannels that served as quarries during the two construction phases and the building site is short (75 m for the most distant walls), with a maximum elevation difference of 10 m. In contrast to the Iberian Period's use of less resistant and more easily extracted sandstones (sampling points A, B, D, E, F), it is evident that the Roman builders chose the sandstones from paleochannel C, which are of higher quality and homogeneity, despite the greater technical difficulty involved in extracting large blocks. This selective use of the best quarries by the Romans has been highlighted by [36] in constructions in northeastern Spain. Other authors, refs. [37,38], have also pointed out the use of high-quality quarries in southern Gaul and Dacia, respectively, beginning in the Roman Period. This is interpreted as evidence of improved management of construction resources under a centralized political authority and a desire for aesthetic distinction compared to pre-Roman constructions. In the case of La Vispesa, we only have a minimal portion of the Roman building walls, making it difficult to assess whether the exploitation of paleochannel C was sufficient to complete the project or to determine the volume of rock extracted. In any case, the presence of extraction marks in the quarry (Figure 8c,d), prepared for continued exploitation, may suggest that there was a sufficient outcrop of this sandstone layer to meet the construction needs.

In semi-arid climates [39], the processes of wetting and drying in sandstone (hydroclasty), combined with salt crystal growth from saline solutions precipitating between the grains (haloclasty), are the main factors contributing to granular disintegration, as well as spalling and flaking, which are common in this lithology [40]. But lithology is not the only factor to be considered to assess weathering processes. It is also important to consider specific microenvironmental factors which can enhance certain differential processes. The position and orientation of the building material significantly influence the penetration of moisture into the rock. Blocks located in lower positions are more affected by the upward movement of water and salts through capillarity. As a result, their degree of deterioration is greater—even though they may be of the highest quality. This may explain the differences in strength observed between the ashlar of wall X, which are more affected by weathering (Figure 6c), and those of wall D. Even in wall D, however, the ashlar at the base (Figure 6e) highlight how the position contributes to greater degradation. Naturally, these same effects are present in the original quarries, where the base of the outcrop is subjected to more intense weathering due to capillarity (Figure 8f), leading to the formation of basal tafoni.

The orientation also plays a decisive role in the degree of weathering. The southwest and southeast orientations appear to be more vulnerable to wetting and drying, haloclasty, and even dissolution, contributing to spalling and granular disintegration. In contrast, the northeast orientation is less affected by these processes. To test this effect, samples MsW and MdE were taken from the same ashlar, oriented west and east, respectively. However, the strength results were identical, indicating the good quality of the rock. Many geomorphological studies have utilized differences in R values and UCS, along with the associated weathering rates, as chronological indicators. Ref. [41] proposes that the degree of weathering measured on rock surfaces using a Schmidt hammer can provide numerical data and serve as an additional dating method. This approach has proven valuable across various lithologies and geomorphological settings [42,43], provided that the data is cross-validated with other dating techniques [38]. For example, refs. [44,45] applied this method to study Holocene moraine blocks in Norway and New Zealand, respectively. In Spain, refs. [13,46] have implemented this method in glacial environments. Ref. [14] have used it to establish phases of block falls on semi-arid slopes, such as those in Los Monegros (Spain), supported by the chronological framework provided by geoarchaeological studies.

This raises the question of whether the notable differences in weathering values observed in the walls of La Vispesa could be attributed to the varying ages of the constructions. If this were the case, it would be reasonable for the Iberian walls to exhibit lower UCS values. However, the minimal chronological gap between the two successive phases of occupation does not appear sufficient to fully account for the disparities in the physical and chemical weathering of the two groups of rocks. As we have indicated, the homogeneity in the composition of the sandstones does not appear to influence the degree of weathering. In any case, the observed differences may be related to the degree of fracturing and subtle granulometric variations. Both Sample C from the paleochannel and the large Roman ashlar blocks exhibit the optimal combination, allowing them to be less affected by weathering.

## 5. Conclusions

The hill of La Vispesa represents a geomorphological type that is very common regionally, and the evolutionary history leading to its current form is well understood. The presence of a deposit corresponding to a phase of Pleistocene pediment, strongly consolidated by a calcrete, has enabled its preservation to the present day. Additionally, the presence of hard paleochannel outcrops mitigates erosive processes by creating a stepped effect in the slope profiles and thereby reducing the gradient. Nevertheless, an evolutionary asymmetry can be observed that is influenced by orientation. The NW and SW slopes

remain protected from significant erosion caused by surface runoff processes, which are more pronounced on the SE slope.

UCS estimates derived from measurements made with a Schmidt hammer (sclerometer) clearly classify the rocks of the La Vispesa walls into two distinct groups, corresponding to different degrees of weathering, which coincide with the chronology provided by the archaeological data.

Broadly speaking, the more weathered Roman walls register UCS values between 57.5 and 60 MPa (wall X), while the less weathered walls range between 73.6 and 77.27 MPa (wall D and the ashlar near the cistern). However, the walls and pavements attributed to the Iberian period, based on archaeological data, show UCS values ranging from 52.5 to 60 MPa. This difference cannot be attributed to the duration of exposure to the elements, because the time interval between the two occupations is not particularly long (200–250 years).

The estimations of UCS values in different outcrops of sandstone channels also reveal the existence of sandstones with high values (75.5 MPa in paleochannel C), which are comparable to the strength values of the Roman wall D. The remaining outcrops yield UCS estimates between 44 and 54.4 MPa, which correspond more closely with the values found in the Illegian walls and the more weathered Roman wall X. These comparisons can provide insight into the varying quality of materials used in the structures of each historical period.

This study contributes to the understanding of the performance of construction materials from the Iberian and Roman periods using uniaxial strength techniques when rock composition data are inconclusive. Additionally, it demonstrates the value of these methods in characterizing materials and understanding the selection and usage practices of lithic raw materials in the past.

**Author Contributions:** Conceptualization J.L.P.-M., E.M.-Z. and A.D.-A.; Methodology, J.L.P.-M. and M.M.S.-V.; Software, M.M.S.-V.; Validation, J.L.P.-M., M.M.S.-V., E.M.-Z. and A.D.-A.; Formal Analysis, J.L.P.-M., M.M.S.-V., E.M.-Z. and A.D.-A.; Investigation, J.L.P.-M., M.M.S.-V., E.M.-Z. and A.D.-A.; Resources, E.M.-Z. and A.D.-A.; Writing—Original Draft Preparation, J.L.P.-M., M.M.S.-V., E.M.-Z. and A.D.-A.; Writing—Review and Editing, J.L.P.-M., M.M.S.-V., E.M.-Z. and A.D.-A.; Visualization, J.L.P.-M. and M.M.S.-V.; Supervision, J.L.P.-M. and M.M.S.-V.; Project Administration, E.M.-Z. and A.D.-A.; Funding Acquisition, M.M.S.-V., E.M.-Z. and A.D.-A. All authors have read and agreed to the published version of the manuscript.

**Funding:** This work is a contribution of the Primeros Pobladores & Patrimonio Arqueológico del Valle del Ebro P3a Research Group. This work has partially benefited from financial and technical support provided by the project PaleoJubierre (IEA-Diputación Provincial de Huesca), research grant RYC2021-031196-I, project ARIDA PID2022-138034OA-I00 (MICIIN-Spain); Gaps and dates: Dinámicas culturales en la prehistoria de la cuenca del Ebro (GAD), Ministerio de Economía y Competitividad PID2020-116598GB-100; and PIUNT G741 and PICT2019-0193 (Argentina).

**Data Availability Statement:** Data available on request from the corresponding authors.

**Conflicts of Interest:** The authors declare no conflicts of interest.

## References

1. Maestro, E.; Domínguez, A. Contribución al estudio de la romanización en La Litera: El yacimiento de La Vispesa (Tamarite de Litera). *Bolskan* **1986**, *3*, 135–167.
2. Maestro, E.; Domínguez, A. El yacimiento de La Vispesa (Tamarite de Litera, Huesca). Testimonio de romanización en territorio ilergete. In Proceedings of the III Congreso Aragonés de Arqueología y Patrimonio (CAPA), Zaragoza, Spain, 14–15 November 2019; pp. 181–193.
3. Maestro, E.; Domínguez, A. Los procesos de iberización y romanización en la comarca de La Litera a través del yacimiento de La Vispesa (Tamarite de Litera, Huesca). Estudio preliminar. *Salduie* **2024**, *24*, 1–25.

4. Domínguez, A.; Maestro, E.; Monforte, A. Criterios de consolidación y conservación del yacimiento de La Vispesa (Tamarite de Litera, Huesca). *Salduie* **2004**, *4*, 363–380. [[CrossRef](#)]
5. Domínguez, A.; Maestro, E.; Paracuellos, P. El yacimiento oscense de La Vispesa: La cerámica de barniz negro helenístico. *Empuries* **2007**, *55*, 125–139.
6. Sancho, C. Geomorfología de la Cuenca Baja del Río Cinca. Ph.D. Thesis, Universidad de Zaragoza, Zaragoza, Spain, 1988.
7. Sancho, C.; Peña, J.L.; Mata, M.P.; González, J.R. Estudio alterológico de la arenisca soporte de las pinturas y grabados de la Roca del's Moros de El Cogul (Lleida). *Cuaternario Geomorfol.* **1994**, *8*, 103–118.
8. Bamford, W.E.; Van Duyse, H.; Nieble, C.; Rummei, F.; Broch, E.; Franklin, J.A.; Atkinson, R.H.; Tarkoy, P.J.; Deere, D.U. Suggested methods for determining hardness and abrasiveness of rocks. *Int. J. Rock Mech. Min. Sci.* **1978**, *15*, 89–97.
9. Aydin, A.; Basu, A. The Schmidt hammer in rock material characterization. *Eng. Geol.* **2005**, *81*, 1–14. [[CrossRef](#)]
10. Aydin, A. ISRM Suggested method for determination of the Schmidt hammer rebound hardness: Revised version. *Int. J. Rock Mech. Min. Sci.* **2009**, *46*, 627–634. [[CrossRef](#)]
11. Katz, O.; Reches, Z.; Roegiers, J.C. Evaluation of mechanical rock properties using a Schmidt Hammer. *Int. J. Rock Mech. Min. Sci.* **2000**, *37*, 723–728. [[CrossRef](#)]
12. Shakesby, R.A.; Matthews, J.A.; Owen, G. The Schmidt hammer as a relative-age dating tool and its potential for calibrated-age dating in Holocene glaciated environments. *Quat. Sci. Rev.* **2006**, *25*, 2846–2867. [[CrossRef](#)]
13. Tomkins, M.; Dortch, J.M.; Hughes, P.D.; Huck, J.J.; Stimson, A.G.; Delmas, M.; Calvet, M.; Pallàs, R. Rapid age assessment of glacial landforms in the Pyrenees using Schmidt hammer exposure dating (SHED). *Quat. Res.* **2018**, *90*, 26–37. [[CrossRef](#)]
14. Peña-Monné, J.L.; Sampietro-Vattuone, M.M.; Picazo-Millán, J.; Alcolea-Gracia, M. Block alignments / talus flatiron stages as response to lithological factors and dynamic slope changes in the Central Ebro Basin, NE Spain. *Quat. Sci. Rev.* **2024**, *340*, 108864. [[CrossRef](#)]
15. Hirst, J.P.P.; Nichols, G.J. Thrust tectonic controls on Miocene alluvial distribution patterns, southern Pyrenees. In *International Association of Sedimentologist Special Publications*; Allen, P., Homewood, P., Eds.; ISSP: London, UK, 1986; Volume 8, pp. 247–258.
16. Jones, S.J. Drainage evolution and terminal alluvial fans, Southern Pyrenees, Spain. *Terra Nova* **2004**, *16*, 121–127. [[CrossRef](#)]
17. Quirantes, J. *Estudio Sedimentológico del Terciario Continental de los Monegros*; Institución Fernando el Católico: Zaragoza, Spain, 1978.
18. Riba, O.; Reguant, S.; Villena, J. Ensayo de síntesis estratigráfica y evolutiva de la cuenca terciaria del Ebro. In *Libro Jubilar J.M. Ríos*; Instituto Geológico Minero de España, Ed.; Instituto Geológico Minero de España: Madrid, Spain, 1983; pp. 131–159.
19. García Senz, J.; Zamorano, M.; Monte, M.; Rico, M.T. *Mapa Geológico 1:50.000 Serie Magna, Hoja 326 (Monzón)*; I.G.M.E.: Madrid, Spain, 1990.
20. Pettijohn, F.J. *Sedimentary Rocks*; Harper: New York, NY, USA, 1957.
21. Domínguez, A.; Maestro, E. Arqueología versus Numismática: Presencia púnica en el yacimiento oscense de La Vispesa (Tamarite de Litera). *Salduie* **2020**, *20*, 65–82. [[CrossRef](#)]
22. Marco, M.F.; Baldellou, V. El monumento ibérico de Binéfar. *Pyrenae* **1976**, *12*, 91–118.
23. Peña Monné, J.L. (Ed.) *Cartografía Geomorfológica Básica y Aplicada*; Editorial Geoforma: Logroño, Spain, 1997.
24. Attanasio, D.; Bruno, M.; Prochaska, W.; Yavuz, A.B. A multi-method database of the black and white marbles of Göktepe (Aphrodisias), including isotopic, EPR, trace and petrographic data. *Archaeometry* **2015**, *57*, 217–245. [[CrossRef](#)]
25. Dilaria, S.; Bonetto, J.; Germinario, L.; Previato, C.; Giroto, C.; Mazzoli, C. The stone artifacts of the National Archaeological Museum of Adria (Rovigo, Italy): A noteworthy example of heterogeneity. *Archaeol. Anthropol. Sci.* **2024**, *16*, 14. [[CrossRef](#)]
26. Tavares, A.; Rocha, F.; Fragata, A.; Costa, A.; Oliveira, M. Comprehensive Overview and New Research on Carbonate Rocks of the Sé Velha Cathedral in Coimbra, Portugal. *Heritage* **2024**, *7*, 5569–5592. [[CrossRef](#)]
27. Niedzielski, T.; Migoń, P.; Placek, A. A minimum sample size required from Schmidt hammer measurements. *Earth Surf. Process. Landf.* **2009**, *34*, 1713–1725. [[CrossRef](#)]
28. Duszyński, F.; Migoń, P. Boulders apron indicate long-term gradual and noncatastrophic evolution of cliffed escarpments, Stołowe Mts., Poland. *Geomorphology* **2015**, *250*, 63–77. [[CrossRef](#)]
29. Miller, R.P. Engineering Classification and Index Properties for Intact Rock. Ph.D. Thesis, University of Illinois, Champaign, IL, USA, 1965.
30. Sancho, C.; Meléndez, A. Génesis y significado ambiental de los caliches pleistocenos de la región del Cinca (Depresión del Ebro). *Rev. Soc. Geol. España* **1992**, *5*, 81–93.
31. Sancho, C.; Meléndez, A.; Signes, M.; Bastida, J. Chemical and mineralogical characteristics of Pleistocene caliche deposits from the Central Ebro Basin, NE Spain. *Clay Miner.* **1992**, *27*, 293–308. [[CrossRef](#)]
32. González-Pérez, J.R.; Peña-Monné, J.L.; Rodríguez Duque, J.I. El tossal de Moradilla (Lleida) en el marco evolutivo del Holoceno superior de la Depresión del Ebro. In *Geoarqueología y Patrimonio en la Península Ibérica y el Entorno Mediterráneo*; Santonja, M., Pérez González, A., Machado, M.J., Eds.; ADEMA: Madrid, Spain, 2005; pp. 383–394.

33. Sampietro-Vattuone, M.M.; Peña-Monné, J.L.; Montón-Broto, F.; Rodanés-Vicente, J.M.; Alcolea-Gracia, M.; Seguí-Barrio, S. Evolutionary model and palaeoenvironmental interpretation of the La Codera archaeological complex (Ebro Basin, NE Spain). *J. Archaeol. Sci. Rep.* **2024**, *53*, 104326. [[CrossRef](#)]
34. Burillo, F.; Gutiérrez, M.; Peña Monné, J.L. La Geoarqueología como ciencia auxiliar. Una aplicación a la Cordillera Ibérica Turolense. *Rev. De Arqueol.* **1983**, *26*, 6–13.
35. Peña-Monné, J.L.; Sampietro-Vattuone, M.M.; Picazo-Millán, J.V. Late Quaternary palaeoenvironmental controls on concentric talus evolution in the Central Ebro Basin (NE Spain). *Environ. Earth Sci.* **2022**, *81*, 422. [[CrossRef](#)]
36. Gutiérrez García-M, A. Roman quarries in the northeast of Hispania (modern Catalonia, Spain). In Proceedings of the IX ASMOSIA Conference, Tarragona, Spain, 8–13 June; 2009; pp. 665–679.
37. Bessac, J.C. Influences de la conquête romaine sur le travail de la pierre en Gaule méditerranéenne. *J. Rom. Archaeol.* **1988**, *1*, 57–72. [[CrossRef](#)]
38. Cetean, V.; Pețan, A.; Stancu, M. Historical Use of the Ashlar Limestone at Piatra Roșie Dacian Fortress; Interdisciplinary Approach in a World Heritage Site. *Sustainability* **2022**, *14*, 11818. [[CrossRef](#)]
39. Goudie, A.S. *Arid and Semi-Arid Geomorphology*; Cambridge University Press: Cambridge, UK, 2013.
40. Young, R.W.; Wray, R.A.L.; Young, A.R.M. *Sandstone Landforms*; Cambridge University Press: Cambridge, UK, 2009.
41. Matthews, J.A.; Winkler, S. Schmidt-hammer exposure-age dating: A review of principles and practice. *Earth-Sci. Rev.* **2022**, *230*, 104038. [[CrossRef](#)]
42. Goudie, A.S. The Schmidt Hammer in geomorphological research. *Prog. Phys. Geogr.* **2006**, *30*, 703–718. [[CrossRef](#)]
43. Goudie, A.S. The Schmidt Hammer and Related Devices in Geomorphological Research. In *Methods in Geomorphology*; Shroder, J., Switzer, A.D., Kennedy, D.M., Eds.; Academic Press: San Diego, CA, USA, 2013; pp. 338–345.
44. Matthews, J.A.; Shakesby, R.A. The status of the ‘Little Ice Age’ in southern Norway: Relative age dating of Neoglacial moraines with Schmidt Hammer and lichenometry. *Boreas* **1984**, *13*, 333–346. [[CrossRef](#)]
45. Winkler, S. The Schmidt Hammer as a relative-age dating technique: Potential and limitations of its application on Holocene moraines in Mt Cook National Park, Southern Alps, New Zealand. *N. Z. J. Geol. Geophys.* **2005**, *48*, 105–116. [[CrossRef](#)]
46. De Marcos, J.; Úbeda, J.; Andrés, N.; Palacios, D. A combination of cosmogenic and Schmidt hammer exposure age dating in the study of the deglaciation timing of Sierra de Guadarrama National Park (Spain). *Geogr. Ann. Ser. A (Phys. Geogr.)* **2022**, *104*, 70–89. [[CrossRef](#)]

**Disclaimer/Publisher’s Note:** The statements, opinions and data contained in all publications are solely those of the individual author(s) and contributor(s) and not of MDPI and/or the editor(s). MDPI and/or the editor(s) disclaim responsibility for any injury to people or property resulting from any ideas, methods, instructions or products referred to in the content.